Author Manuscript

Author Manuscript

Author Manuscript

Author Manuscript

HHS Public Access

Author manuscript

Adv Healthc Mater. Author manuscript; available in PMC 2019 July 01.

Published in final edited form as:

Adv Healthc Mater. 2018 July ; 7(14): e1800252. doi:10.1002/adhm.201800252.

Quantum Dot-Dye Conjugates for Biosensing, Imaging and Therapy

Sungwook Jung and **Xiaoyuan Chen**

Laboratory of Molecular Imaging and Nanomedicine, National Institute of Biomedical Imaging and Bioengineering, National Institutes of Health, Bethesda, Maryland 20892, USA.

Abstract

Quantum dots (QDs) are nanoscaled fluorescent materials with superior optical properties, making them useful tools to investigate biological phenomena or to diagnose various diseases. Added values on the intrinsic properties of QDs, a strategy to conjugate dyes on the surface of QDs offers new opportunities since the coupling between QD and dye can be designed to allow Förster resonance energy transfer (FRET) and/or electron transfer (eT). These processes are accompanied by the change of QD and/or dye fluorescence and subsequent photochemical reactions (*e.g.* generation of $^1O_2$). Based on the change of fluorescence signals by the interaction with biomolecules, QD-dye conjugates have been exploited as biosensors for the detection of pH, O_2, NADH, ions, proteases, glutathione, and micro-RNA. QD-dye conjugates also can be modulated by the irradiation of external light; this concept has been demonstrated for fluorescence super-resolution imaging as photoactivatable or photoswitchable probes. When QDs are conjugated with photosensitizing dyes, the QD-dye conjugates can generate $^1O_2$ in a repetitive manner for better cancer treatment, also, can be available for approaches using two-photon excitation or bioluminescence resonance energy transfer mechanism for deep tissue imaging. Here, the recent advances in QD-dye conjugates, where FRET or eT produces fluorescence readouts or photochemical reactions, are reviewed. Various QD-dye conjugate systems and their biosensing/imaging and photodynamic therapeutics are summarized.

Short summary

Conjugation of dyes on QDs offers new opportunities due to FRET (A) and/or electron transfer (B) between the two. QD-dye conjugates have been exploited as biosensors over pH, O_2, NADH, ions, proteases, glutathione, and microRNA. Photomodulation of QD-dye conjugates has been demonstrated for fluorescence super-resolution imaging. QD-photosensitizing dye conjugates can generate $^1O_2$ in a repetitive manner for better cancer treatment.

Table of contents

shawn.chen@nih.gov.

Author Manuscript Author Manuscript Author Manuscript Author Manuscript

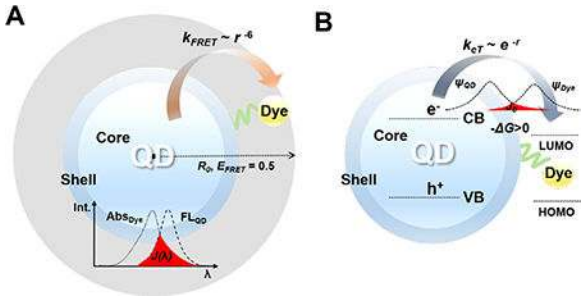

1. Introduction

1.1 Quantum Dots (QDs) and QD-Dye Conjugates

Quantum dots (QDs), colloidal semiconductor nanocrystals, are one of the most promising and versatile nanoparticles (NPs), especially in advancing biology. The characteristics of QD for biological applications over conventional organic dyes include the large (two-photon) absorption coefficient, high brightness (1 – 2 orders of magnitude brighter than that of single organic dye), symmetric and narrow emission profile, and robustness to photobleaching.[1] The photostable and bright properties of QDs allows long-term acquisition of fluorescence with a high signal-to-noise ratio, which can be taken advantage of for cellular labelling,[2] single molecule tracking,[3] and *in vivo* imaging.[4] QDs have broad absorption spectra, which allows for simultaneous and multiplexed emissions under single light source. The narrow and symmetric emission spectra of QD are optimal for unmixing the fluorescence signals. The emission wavelength range for QD spans from UV to visible, infrared and then opens a broad spectral window for multiplexed imaging.[2c, 4c, 4d] Large two-photon cross sections of QDs leads to deep tissue bioimaging.[5] Beyond these inherent optical properties of QDs, conjugation of QDs with dye molecules can add biological value of the materials by interacting their fluorescent properties with those of dye molecules, which causes Förster resonance energy transfer (FRET) and/or electron transfer (eT) processes. Due to the nanometer size of typical QDs, QDs can be conjugated with multiple copies of the dye molecules. The multivalent conjugation can lead to high optical sensitivity and chemical stability in biological studies. Furthermore, QD-dye conjugates offer the distinctive ability to produce discrete readouts, which are results from both the conjugated ratio of a QD donor to a dye acceptor and the distance of QD-dye. QD-dye conjugates also have a great potential for fluorescence super-resolution imaging as photoactivatable or photoswitchable probes, because conjugated dyes can control the intensity of QD fluorescence by the light-induced reaction of dyes. In the context of nanomedicine, the subsequent chemical reactions (*e.g.*, generation of $^1O_2$) after the transfer phenomenon in QD-dye conjugates lead to the specific disease therapeutics in a repetitive manner. The versatility of QD-dye conjugates has been verified for the last decade by the support from advanced QD synthesis and surface chemistry for ideal conjugations between QD and dye molecules.[6] Herein, we summarize the advance created on conjugating QDs and dye molecules for FRET and/or eT from the viewpoint for biological applications. Our goal is to provide readers how QDs are continuously accelerating the appearance of novel biosensor/bioimaging and therapy by

Author Manuscript Author Manuscript Author Manuscript Author Manuscript

conjugating dyes on their surfaces and exploiting release or photochemical reactions of the dyes.

1.2 Förster Resonance Energy Transfer and Electron Transfer (eT)

Förster resonance energy transfer (FRET) and electron transfer (eT) between QD and dye molecules are arguably the most preferred approaches to change fluorescence signals or to induce chemical reactions for bioapplications (Figure 1). FRET pair consists of a donor and an acceptor, where QD mainly acts as a donor and conjugated dye accepts the QD energy. FRET occurs when a luminescent donor in the excited state (D*) and a light absorbing acceptor in the ground state (A) are reasonably interacted as approximated point dipoles.[7] FRET produces a donor in the ground state (D) and an acceptor in the excited state (A*) without photon or physical engagement (Equation 1).

$$D^* + A \rightarrow D + A^* \quad (1)$$

The FRET efficiency (E_{FRET}) is given by Equation 2. It can be seen from this equation that R_0 represents Förster distance; the donor-acceptor distance where E_{FRET} is 50%. r is the distance between the donor and the acceptor and N is the number of conjugated acceptors.

$$E_{FRET} = NR_0^6/\left(NR_0^6 + r^6\right) \quad (2)$$

Since energy is non-radiatively transferred in a distance-dependent manner (FRET rate ~ r^{-6}),[7–8] the donor-acceptor pair should be in close proximity, and the upper limit of the distance for FRET is considered to be ~10 nm.[7, 9] However, since the size of QDs and most dyes satisfies the distance scale, thus, QD-dye conjugates can achieve FRET pairs.[8–9] Transition dipoles of both the donor and acceptor should be orientated favorably to each other, which induces energetic resonant transitions, and also FRET channel should be competitive to other channels in taking the donor energy.[10] R_0 is determined by this donor-acceptor configuration, and serves as a standard of the intrinsic FRET capability of a specific donor-acceptor construct. R_0 is defined by Equation 3, where Φ_D is the fluorescence QY of the donor, n is the refractive index of surrounding medium, κ^2 is the orientation factor, and $J(\lambda)$ is the spectral overlap integral.

$$R_0^6 = \left(8.79 \times 10^{-28} mol\right) n^{-4} \Phi_D \kappa^2 J\left(\lambda\right) \quad (3)$$

Enhanced spectral overlap between donor emission and acceptor absorption results in a large R_0 due to much resonant dipole transitions. Since a donor with high QY has low competition channels and an acceptor with large molar absorption coefficient induces the direct excitation, the R_0 also increases.[8, 10] In-depth information on FRET for QD can be found in different review articles.[11]

Author Manuscript Author Manuscript Author Manuscript Author Manuscript

eT involves electron-hole separation, which can be exploited for signals in many of the same ways like FRET because the charging for QD triggers fluorescence quenching. In contrast to FRET mechanism which is dependent on spectral overlap, eT takes root in Marcus theory and requires orbital overlap that reduces exponentially as donor-acceptor distance (r) increases (eT rate ~ e^{-r}).[12] This one-electron phenomenon occurs between an excited donor (D*) and acceptor (A), and depends on the inner and outer reorganization of the donor-acceptor construct and the solvent.

$$D^* + A \rightarrow D^{\bullet +} + A^{\bullet -} \quad (4)$$

The rate of eT can be expressed in Equation 5.

$$k_{eT} = \frac{\frac{2\pi}{\hbar} J_0^2 \exp\left[-\beta\left(r - r_0\right)\right]}{\sqrt{4\pi\gamma(r)k_B T}} \exp \frac{-(\Delta G(r) + \gamma(r))^2}{4\gamma(r)k_B T} \quad (5)$$

where r_0 is r when donor meets acceptor, λ is the reorganization energy, β is the orbital coupling, J_0 is the matrix element for donor/acceptor electronic coupling, ΔG is the change of free energy (driving force), $\hbar$ is the Planck's constant divided by 2π, T is the temperature, and k_B is the Boltzmann constant, respectively.[13] The rate constant of eT (k_{eT}) increase with increasing driving force ($-\Delta G_0$), and then decreases when the driving force is greater than the reorganization energy (λ). The rate is also modulated by the electronic coupling factor (J_0^2) between the initial and final states.[14] The independency for spectral overlap in eT mechanism can be an advantage for multiplexed biosensing/imaging because several QDs with different colors can be simultaneously quenched by only one type of dye acceptor.[15] For eT from of QD to dyes to quench QD fluorescence, energy of LUMO of the dyes should lie between conduction band edge and valence band edge of the QDs, and that the dyes be located in the proximity of the QD.[16] Various biosensing/imaging based on the use of QD fluorescence by a variety of eT dyes have been recently reported.[15b, 17] A recent review broadly covered the electronic process between QD and proximate dyes.[14]

2. Cell-based biosensors

2.1 pH Sensors

pH regulation is crucial for normal physiology and cell metabolism and function.[18] Given its important role and the disruption of homeostasis when not controlled, the pH of the intracellular fluid and the extracellular fluid need to be maintained at a constant level by high buffering capability and ion transporting property.[18–19] Several groups have exploited QD-based approaches to measure cellular pH.[20] Medintz *et al.* reported that QD-dopamine conjugates were pH-responsive by the redox abilities of the conjugated dopamine dye (Figure 2).[20a] The surface of CdSe/ZnS QDs (λ_{em} = 550 nm) were coated with hexahistidines that are covalently attached by dopamines. Oxidized dopamine-quinone

Author Manuscript Author Manuscript Author Manuscript Author Manuscript

functions as an acceptor of electron. At low pH, a small amount of oxidized dopamine was produced, which induced marginal quenching. As pH increased, dopamine was oxidized and provided as a non-radiative channel to quench QD fluorescence. They microinjected QD-dopamine conjugates to the cytosol of COS-1 cells. As intracellular pH increased by the change of medium with pH 11.5, the fluorescence of QD-dopamine conjugates was quenched by eT from the photoexcited QD to dopamine quinone in a pH-dependent manner over the range pH 6.6 – 11.5 for 1 h. Susumu *et al.* devised QD conjugates to sense extracellular pH.[20b] They prepared ZnSe/$Cd_yZn_{1-y}S$/ZnS and $Cd_xZn_{1-x}Se$/$Cd_yZn_{1-y}S$/ZnS QDs (λ_{em} = 410 – 530 nm). The surface of QD was decorated with fluorescein isothiocyanate (FITC) which is a pH-sensitive dye, forming FRET pairs. Ratiometric fluorescence intensity, defined as I_{QD}/I_{FITC}, of QD-FITC conjugates increased linearly as pH varied from 3 to 7.5. QD-FITC conjugates modified by membrane targeting peptides demonstrated pH-monitoring capability in extracellular environments. Fluorescence intensity-based pH sensors can be perturbed by their scattering, sample turbidity, and autofluorescence.[21] Alternatively, fluorescence lifetime (FLT) technique for pH sensing has drawn attention due to its independence on the perturbations. Tang *et al.* demonstrated high pH-response of FLT in their QD conjugates in the near-infrared (NIR) range.[20c] CdTeSe/ZnS QDs (λ_{em} = 750 nm) were functionalized with cysteamine and then covalently conjugated with pH-sensitive NIR carbocyanine dye LS662 (pKa = 5.2). The absorption peak of the dye shifted from 750 nm to 520 nm with increasing pH. QD750-LS662 conjugates had high pH response: with increasing pH, FLT decay profile of the QD fluorescence showed a sigmoidal increase from 12 ns (pH < 5) to 29 ns (pH >7).

2.2 Sensors for Metal Cations

The concentration of intracellular ions is important to maintain cellular homeostasis. QD-dye conjugates have been used for sensing various ions.[22] Although small molecule indicators for Ca^{2+} are useful tools for investigating intracellular signaling, they show no reliable detection of local Ca^{2+} entry. Zamaleeva *et al.* reported QD biosensors which penetrate cells, in order to detect intracellular local Ca^{2+}.[22c] They conjugated CdZnSe QD (λ_{em} = 565 nm) to CaRuby, a Ca^{2+} indicator with red emission. R_0 was calculated as 45 Å. The QD was also modified with 5 – 10 cell penetrating peptides (CPP) originated from hadrucalcin to facilitate its cytosolic entry. QD-CaRuby conjugates could detect Ca^{2+} in the range of 3 to 20 μM. QD-CaRuby conjugates were incubated with baby hamster kidney cells (BHK-21) that express Ca^{2+}-permeable N-methyl-D-aspartate receptor (NMDAR) constructs. After the injection of an NMDAR agonist (glutamate and glycine) which induced the Ca^{2+} influx, QD-CaRuby conjugates sensed heterogeneous intracellular Ca^{2+}. When imaged with total internal reflection fluorescence (TIRF) microscopy, these QD-CaRuby conjugates displayed a punctate cytoplasmic distribution; in monitoring of fluorescence in the punctate, they could confirm that local Ca^{2+} signals were evoked by NMDAR activation. Zn^{2+} is found in almost every tissue of the body and exists as chelated form. After release, Zn^{2+} tailors several ion channels and receptors for the biological modulations. Wu *et al.* reported a FRET-based ratiometric sensor to detect Zn^{2+} by dual colored QDs as donors, silica shell as a spacer, and meso-tetra(4-sulfonatophenyl)porphine dihydrochloride (TSPP) as an acceptor.[22b] Green fluorescence emitting QD (λ_{em} = 512 nm) and yellow fluorescence emitting QD (λ_{em} = 572 nm) were coated with amine-modified silica layers.

Author Manuscript Author Manuscript Author Manuscript Author Manuscript

Negatively charged TSPP chelator was attached to the silica layer by electrostatic interaction. In the absence of Zn^{2+}, FRET arose from the GQD to TSPP, producing the signal with low green and high yellow emission ($I_G/I_Y = 0.67$). In the presence of Zn^{2+}, ion chelation changed the absorption in the Q-band of the TSPP, which suited well for the FRET with YQDs, enhancing the QD fluorescence ratio (I_G/I_Y) up to 1.6 within ~30 min. QD-TSPP conjugates could detect Zn^{2+} of 0.3 – 6.0 μM under physiological conditions. They demonstrated the Zn^{2+}-selective change of I_G/I_Y of the conjugates over various other cations including Ca^{2+}, Fe^{3+} and Cu^{2+}. The ratiometric QD-TSPP conjugate was also used to detect Zn^{2+} in live human colon carcinoma cells (HCT116). After the treatment with 6.0 μM $ZnCl_2$, QD fluorescence ratio increased from 0.38 to 1.4 over time. This ratiometric probe using alternative quenching of two colors enhances the dynamic range of biological signals, which can lower the limit of detection, however, for the *in vivo* real-time applications, it is required to shorten current response time (~30 min) of such probes.

2.3 Oxygen Sensors

The concentration of O_2 is an especially important indicator of tumor health,[23] due to the hypoxic characteristics of tumor microenvironment.[24] Therefore, the development of reliable O_2 sensors to detect biological environments has attracted great attention. However, the detection for dissolved gases in cells and tissues is a challenge, and real-time monitoring of the of O_2 dynamics based on fluorescence signal has been impeded by the dependency on organic dyes.

McLaurin *et al.* designed QD-osmium(II) polypyridyl (QD-Os(II)PP) constructs for the detection of oxygen in biological environments.[25] CdZnSe/CdZnS QDs (λ_{em} = 525 or 549 nm) were conjugated with Os(II)PP by the formation of amide bonds. The Os(II)PP dyes possess broad absorptions, making them favorable FRET acceptors from QD donors. The photoluminescence of the conjugated Os(II)PP increased from 1.3% to 23% while QD fluorescence was attenuated; E_{FRET} reached 67%. With the irradiation of NIR light (λ_{ex} = 920 nm), FRET occurred in QD-Os(II)PP conjugates, due to the large two-photon absorption cross-section in QDs. Upon exposure to 1 atm O_2, photoluminescence from the Os(II)PP dye was quenched by 23% while the QD fluorescence was unaffected. However, there were no further experiments to showcase bioapplication of the QD-Os(II)PP. Visualization of O_2 in real-time is of great interest due to its critical role in cellular metabolism. Ingram *et al.* presented a ratiometric O_2 sensing technology using QD conjugates.[26] They conjugated QD (λ_{em} = 590 nm) with an oxygen-quenching platinum(II)-octaethylporphine ketone (PtOEPK) to form FRET pairs, where PtOEPK quenched fluorescence of QD and emitted *via* FRET. QD-PtOEPK conjugates were embedded within an inert polyvinyl chloride matrix. The QD conjugate-loaded polymer was deposited to glass substrate or opto-pod matrix allowed the measurement of interstitial O_2 concentration in biological microdomains of rat hippocampal brain tissue during seizure; the temporal resolution was several hundred milliseconds.

2.4 $NAD(P)^+$ Sensors

1,4-nicotinamide adenine dinucleotide (phosphate), $NAD(P)^+$, is a coenzyme found in all cells, which plays an important role in cell metabolism. $NAD(P)^+$ is engaged in redox

Author Manuscript Author Manuscript Author Manuscript Author Manuscript

reactions, transferring electrons from one reaction to another. Numerous enzymes carry out their functions with the electron transporter by $NAD(P)^+$. Freeman *et al.* reported the design of QD-Nile blue conjugates to detect NADH. They modified CdSe/ZnS QDs (λ_{em} = 635 nm, diameter = 7.3 nm) with bovine serum albumin (BSA), and Nile blue was conjugated to BSA layer *via* covalent bond (Figure 3).[27] Nile blue acted as an electron mediator to oxidize NADH cofactors. QD-Nile blue conjugate was incubated with HeLa cells in a growth medium containing D-glucose. Fluorescence intensity of QD-Nile blue conjugate increased over incubation time, as a result of NADH generated by cell metabolism in the presence of D-glucose. In a control experiment, Hela cells incubated with QD-Nile blue conjugate showed no recovery of QD fluorescence when treated with taxol. They demonstrated the feasibility of such QD conjugates for screening anti-cancer agents and probing the effect of drugs on cellular metabolism, based on NAD^+-dependent biocatalytic transformations.

2.5 Protease Sensors

The secretion of active proteases is critical biological phenomenon relevant to cellular plasma membrane. Proteases are associated with the maintenance of cellular health as well as disease progression such as cancer spread. For this reason, significant efforts have been devoted to the diagnosis of cancers or development of drugs by targeting cancer-specific proteases. Shi *et al.* reported QD FRET sensors for monitoring the proteolytic activity of extracellular matrix metalloproteinases (MMPs) in normal and cancer cells.[28] They labeled RGDC peptide with rhodamine (Rh) and prepared QD-Rh conjugates by exchanging CdSe/ZnS QDs (λ_{em} = 545 nm) with the Rh-labeled RGDC peptides. Since Rh served as acceptors, the conjugation quenched the QD fluorescence by FRET. In the solution of collagenase, a MMP, peptide molecules were enzymatically cleaved, thus, Rh molecules no longer could play the FRET acceptor role in the system. As a result, the QDs recovered their emission. When the QD Rh conjugates were incubated with the culture medium of breast cancer cells (HTH 126) which secreted active MMPs, re-emission of QD donor was observed, while there was no noticeable change of the QD emission in the medium from control cells (HT125). Chung *et al.* developed a multifunctional QD probe to image the activity of MMP on cellular membrane.[29] They used bent peptide sequences which enable FRET pairs position with the close distance to allow high FRET (Figure 4). N-terminus of the peptide was appended to CdSe/ZnS QD (λ_{em} = 525) *via* a hexahistidine sequence, while the C-terminus was coupled to Cy3 *via* maleimide-cysteine reaction. In the middle of the peptide, there was an AHLR substrate sequence to be recognized by MMP and an RGD moiety for targeting cellular membrane. active MMP can cleave this substrate, which results in re-emission of QD donor and cell penetration by remaining peptide sequences with positive charge. QD-Cy3 conjugates were incubated in MDA-MB-231 cells (high expression of MT1-MMP) and HeLa cells (MT1-MMP deficient). Compared to HeLa cells, MDA-MB-231 cells showed higher change of QD FRET, and also had significantly higher internalized uptake the QDs. This study is a prime example to represent the advance of smart multifunctional QDs, where single biological phenomenon (*e.g.*, protease activity) induces two kinds of responses (*e.g.* change of E_{FRET} and cellular uptake).

Author Manuscript Author Manuscript Author Manuscript Author Manuscript

The second NIR region (NIR-II, λ = 1,000 – 1,700 nm) has risen up as a novel optical window which distinctively decreases light scattering and thus allows high sensitivity for deep tissues.[30] Jeong *et al.* reported MMP-activatable NIR-II emitting QD probes that exhibit fluorescence in tumor microenvironment.[17d] PbS/CdS/ZnS QDs (λ_{em} = 1,200 nm) were synthesized and conjugated with methylene blue (MB) that quenches QD fluorescence *via* eT (Figure 5). Peptide sequence for the protease-induced cleavage was located between the donor-acceptor pair. In a colon cancer (AOM/DSS) mouse model, they demonstrated the activation of QD fluorescence specifically at tumor sites; this signal was enhanced by 3-fold within 10 min. In an optical phantom experiment, they analyzed fluorescence signals of the QD-MB conjugate over conventional dye (Gehence 750) with emission in the first near-infrared (NIR-I) region. With increasing the thickness of phantom from 0 to 5 mm, the fluorescence of NIR-I dye became more blurred as compared to that of QD-MB conjugates due to the distinguishably smaller light scattering in NIR-II window. They demonstrated deep tissue imaging capability of QD-dye conjugates. For more discussion and examples on protease sensors, interested readers are referred to a recent review.[31]

2.6 Glutathione Sensors

Reduced glutathione (GSH) is the most abundant cellular thiol (1 to 15 mM) and plays a critical role in cellular redox reactions.[32] Unregulated concentration of GSH induces a variety of diseases including cancer and heart diseases.[33] However, conventional organic dyes cannot ensure the consistent detection of GSH with sufficiently high sensitivity. Several studies demonstrated that QD fluorescence can be quenched by FRET or eT from QD to conjugated quenchers, and that the QD conjugates are useful for selective and sensitive detection of GSH *via* competitive chelation.[34] Banerjee *et al.* designed GSH activatable probes based on QDs.[34c] They synthesized Mn-doped CdS/ZnS QD (diameter ~ 4 nm), which shows emission at 592 nm by $^4T_1 \rightarrow {}^6A_1$ transition of the doped Mn ion. The QD was covalently conjugated with dopamine *via* carbon disulfide linker; this conjugated dopamine transferred its electron to QDs, inducing significant quenching of QD fluorescence (~53 times). GSH induced the recovery of QD fluorescence by 25 times in the QD-dopamine solution, because GSH reduced the disulfide and detached the conjugated dopamine. With increasing concentration of GSH from 0 to 10 mM, the fluorescence of QD-dopamine conjugates linearly increased. Lie *et al.* reported the response of QD-methyl viologen (MV^{2+}) conjugate to GSH.[34d] CdSe/ZnS QDs were exchanged by mercaptoacetic acid and then conjugated with MV^{2+} *via* electrostatic interaction. The eT from QD to MV^{2+} quenched the QD fluorescence. The fluorescence of QD-MV^{2+} conjugates was recovered linearly with increasing the concentration of GSH (0 – 250 μM).

2.7 microRNA Sensors

Various approaches for microRNA (miRNA) detection with high sensitivity and accuracy have been reported, since the dysfunction of miRNA can induce different cancers and cardiovascular diseases.[35] Quantitative reverse transcription-polymerase chain reaction (qRT-PCR), northern blotting, and small RNA sequencing have been exploited for miRNA analysis.[36] However, the development of simple, sensitive, multiplexed, and homogeneous strategy for clinical diagnostics of miRNA is still challenging. QD-based FRET probes have demonstrated their superior optical capability for the challenging genetic sensing factors:

Author Manuscript Author Manuscript Author Manuscript Author Manuscript

high brightness, multicolor, and specific readout.[22c, 37] Su *et al.* reported QD probes for the detection of sensitive miRNA.[37b] CdTe/CdS QDs (diameter ~ 3 nm, λ_{em} = 580 nm) were synthesized in aqueous solution using 3 mercaptopropionic acids (MPAs). MPAs on the surface of QDs were exchanged by thiolated DNAs which can hybridize with target miRNA-21. After the addition of miRNA-21 and black hole quencher 2 (BHQ2), sandwiched constructs were formed, quenching of QD fluorescence by FRET from QD to BHQ2 QD fluorescence proportionally decreased in the miRNA-21 concentration from 1 fM to 10 nM. In the absence of target miRNA-21, DNA QDs showed no significant change of the fluorescence since the QDs cannot conjugate with BHQ2.

3. Photoactivatable or Photoswitchable Probes

QDs have been used as super-resolution imaging probes. Hoyer *et al.* exploited blue-shifting PL property of QDs by photooxidation process[38]. Upon light irradiation to induce the QD-blueing, a fluorescent imaging detector recorded PL of only a small number of QDs emitting in a specific wavelength range. High-power irradiation (~10 kW/cm^2) of a light source is required to trigger QD-blueing, however, such as requirement can obstruct *in vivo* applications. Based on super-resolution optical fluctuation imaging (SOFI)[39], Dertinger *et al.* showed sub-cellular PL images using QDs. This mathematic method can improve the spatial resolution of fluorescence images by using temporal correlation among CCD pixels which record PL blinking of QD. However, QD blinking is not controllable but random alteration[40], and also blinking of neighboring QDs can interfere with each other[17a, 41]; this can produce distorted super-resolution images. Modulation of QD fluorescence by light irradiation can be used for super-resolution imaging especially in reversible saturable or switchable optical fluorescence transitions (RESOLFT) and far-field nanoscopy based on photoactivated localization microscopy (PALM). The fluorescent transition between a dark state and a bright state allows localization of a single QD with ~1 nm preciseness.[42] This will lead to multiplexed super-resolution imaging beyond diffraction limit in cellular imaging level due to the broad range absorption property of QD. Unlike photochromic organic dyes, it is challenging to accomplish the modulation of QD fluorescence with external photons. Photophysical reaction between QD and conjugated dyes in the close proximity is typically exploited to modulate QD fluorescence. If QDs are decorated with dyes that possess a photochromic or photoresponsive moiety, irradiation chemically change the conjugated dyes, as a result, modulates the QD fluorescence.[43] QDs conjugated with photochromic spiropyrans[44] or diheteroarylethenes[45] demonstrated controlled E_{FRET} by different states of photochromic moieties, which in turn modulated the fluorescence of QD. QDs appended with a photocleavable ortho-nitrobenzyl moiety[46] or polyviologen[47] displayed photoactivation. Han *et al.* designed photoactivatable QDs using photolytic reaction of *ortho*-nitrobenzyl (ONB) group. CdTe/CdS QDs (λ_{em} = 520 nm, diameter = 6 nm) were coated with 4,5-dimethoxy-1-(2-nitrophenyl)ethyl (DMNPE).[46b] QD-DMNPE conjugates showed the quenching of fluorescence (400-fold reduction) *via* charge transfer mechanism as verified in time-resolved analysis. UV irradiation (λ = 365 nm, 2 mW/cm^2) increased the intensity of QD fluorescence by the photolytic release of ONB byproduct (nitroketon). QD-DMNPE conjugates were incubated in NIH 3T3 fibroblast cells. UV irradiation recovered the fluorescence of intracellular QDs. Therefore, they demonstrated

Author Manuscript Author Manuscript Author Manuscript Author Manuscript

QD-based photoactivatable probes which have the potential to confer an increase of resolution in fluorescence bioimaging. Zhu *et al.* demonstrated photoswitching of QD fluorescence based on photochromic capabilities of conjugated dyes.[44] They functionalized the surface of CdSe/ZnS QD (λ_{em} = 546 nm) with thiolated spiropyrans. UV irradiation changed the dyes to isomeric merocyanines that absorb strongly visible light, inducing FRET between the QD and the merocyanine. QD-spiropyran conjugates exhibited light-induced reversible photochromism like free photochromic dyes. eT mechanism was also exploited for the photomodulation of QD fluorescence.[15b, 48] Bang *et al.* reported fluorescence modulation of QDs by eT from thiolated acridine-1,8-dione derivative surface ligands (ADDs).[49] The surface of as-synthesized CdSe, type-I CdSe/CdS/ZnS, and type-II CdTe/CdSe QDs were exchanged by ADDs. The LUMO level of the ADD is higher than the conduction band edge of the QD, electrons of ADDs are thus transferred to the QD, resulting in negatively charged QDs of which fluorescence could be quenched with high efficiency *via* Auger non-radiative recombination.[48, 50] UV irradiation (λ_{ex} = 365 nm) which can excite ADD quenched the fluorescence of QD-ADD conjugates down to 2% compared with the unconjugated QDs. When irradiated by visible light, QD-ADD conjugates recovered the fluorescence up to 84%. Reversible fluorescence switching of QD-ADD conjugates was demonstrated in many repeated cycles of UV excitation.

Relatively long irradiation of strong UV is, however, required for the photolytic reaction, photoisomerization, or dye excitation, and QDs usually have stronger UV absorption than the dyes. For that reason, modulation of QD fluorescence is not efficient. To address this, Jung *et al.* reported a visible light-induced modulation of fluorescence in QD-crystal violet (CV) conjugates (Figure 6).[15b] Since CV is intrinsically positively charged, they modified the surface of CdSe/CdS/ZnS QDs (λ_{em} = 560 nm or 620 nm) by negatively charged ligands followed by the preparation of QD-CV conjugates *via* electrostatic interactions between the two. CV quenched QD fluorescence by eT from LUMO of CV to the conduction band edge of QD. The fluorescence of QD-CV conjugates showed fluorescence burst including three stages of (1) quenched “off” by CV conjugation to (2) photoactivated “on” by photodegradation of CVs induced by QD photoelectrons and (3) again to photodarkened “off” by radicals. After incubation with HeLa cells, the intracellular QD-CV conjugates showed photomodulation from “off” to “on” and subsequent “off” by ~10-fold upon the irradiation by visible light. Individual fluorescence dynamics of QD-CV conjugates displayed stochastic photoactivations and photodarkenings. They demonstrated simultaneous multicolor super-resolution localizations based on the stochastic fluorescence burst of QD-CV conjugates, disentangling the QDs 46.6 nm apart.

4. Photosensitizers

Photodynamic therapy (PDT) has grown as a FDA-approved approach for a variety of cancers and demonstrated potential for the treatment of other diseases including cardiac illness and AIDS.[51] A number of nanoparticles have been exploited for enhanced PDT treatment over different diseases.[52] PDT includes a tissue-localizing photosensitizer (PS) which can be activated by light irradiation with a specific wavelength. The PS can be delivered to tissues by systemic or local treatment, but is non-toxic before particular irradiation. In the common concept for PDT, PS in excited triplet state transfers its energy to

Author Manuscript Author Manuscript Author Manuscript Author Manuscript

nearby oxygen molecules in ground triplet state, which forms reactive oxygen species (ROS) including cytotoxic singlet oxygen ($^1O_2$). Due to the highly reactive nature, $^1O_2$ oxidizes a wide range of biomolecules, which causes irreversible tissue damage, and selectively eradicates diseased tissues, which is based on the localized radius of action (< 0.02 μm) followed by its short lifetime (< 0.04 μs).[53] PDT thus can be a method for targeted disease treatment and can avoid systemic side effects that are often a hurdle in traditional chemotherapies. However, PSs generally have poor solubility in water and, as a result, tend to aggregate in biological media. The aggregation can result in reduction of photochemical activity and low cell or tissue penetration. To address this challenge, nanoparticles have been widely studied as promising delivery vehicles of PSs, including gold nanoparticles,[54] ceramic nanoparticles,[55] and QDs.[56] Especially, QDs have large transition dipole moment and thus are strong absorbers,[57] which enable them to act as energy donor agents for PDT. Furthermore, the possibility for energy transfer from QDs to triplet oxygen potentially could induce the generation of ROS to provoke apoptosis in cells.[56b] QDs also meet criteria for desirable PS, including facile and cost-effective synthesis, biocompatibility, targeting ability to specific tissues, reduced self-aggregation, non-toxicity, and high cytotoxicity selectively by light illumination.[56b]

Samia *et al.* reported a facile QD-based system to generate $^1O_2$.[56a] 5 nm CdSe QDs were conjugated with the silicon phthalocyanines (Pc4s). They confirmed the two-step FRET among QD, Pc4, and oxygen molecule.[51b, 56a] They reported that E_{FRET} was 77% in QD-Pc4 conjugates, however, the $^1O_2$ QY was ~5%; this $^1O_2$ generation is not efficient compared with the value of ~40% in only Pc4.[58] They also observed the generation of $^1O_2$ by triplet energy transfer (TET) from QDs to triplet oxygen ($^3O_2$). Yaghini *et al.* explored the generation of ROS directly from PEGylated CdSe/ZnS QDs.[59] Direct $^1O_2$ generation from photoexcited QDs was not reported in this study. However, they found that non-photolytic visible wavelength excitation induced ROS generation with QY of 0.35%, which significantly increased *via* FRET in the QDs conjugated with sulfonated-PCs. Shi *et al.* conjugated electrostatically water-soluble CdTe QDs (diameter = 3.4 nm) with meso-tetra(4-sulfonatophenyl)porphine dihydrochloride (TSPP) as a PS for $^1O_2$ generation.[60] After the deposition of TSPP, the QD conjugates showed ~10-fold enhancement in the extinction coefficient (18,350 M^{-1}) at 355 nm compared to TSPP alone. QD-TSPP conjugates (diameter = 6 – 8 nm) showed strongly quenched PL, suggesting FRET from QD to TSPP. After irradiation by near-UV or visible light, they confirmed strong generation of $^1O_2$ from QD-TSPP conjugates and the QY reached 43%. They established that water-soluble QD conjugates can produce $^1O_2$ with a QY that is sufficiently high for biological applications. Tsay *et al.* attached two kinds of PSs, Rose Bengal (RB) or Chlorin e6 (Ce6), to phytochelatin-like peptides; the modified PSs were decorated to the surface of CdSe/CdS/ZnS QDs which have emission peak at 540 or 620 nm, respectively.[61] They conjugated covalently the PS-peptides to the QDs *via* EDC-NHS chemistry. Depending on QD, PS, ratio of PD to QD, and excitation wavelength, QY of $^1O_2$ generation varied between 9% and 31%. In particular, the efficiency for $^1O_2$ by QD excitation (10%) in QD-Ce6 conjugates was lower than that by direct excitation of Ce6 (31%); this originated from inefficient E_{FRET} of 10% due to donor-acceptor distance (~75 Å). Despite the inefficient FRET, the extinction coefficient of QDs is approximately 10× greater than that of the PSs,

Author Manuscript Author Manuscript Author Manuscript Author Manuscript

which means that large amounts of $^1O_2$ could be generated. Furthermore, this method allows for the control of PS number on the QD, increasing the E_{FRET} up to 50%. Qi *et al.* investigated two-photon excitation (TPE) in QD-PS conjugates to find a solution for tissue penetration problem. They encapsulated CdSe/ZnS QDs (diameter = 5 nm) into amphiphilic polymers (poly(maleic anhydride-alt-1-octadecene) (PMAO)-PEG) for improved biocompatibility and circulation, and then used covalent bond to form robust QD-porphyrin conjugates (diameter = 44 nm) for the generation of $^1O_2$.[62] The biocompatible QD conjugates shows a two-photon absorption cross section values in the range from 800 nm to 1100 nm, which is critical for deep tissue PDT using NIR light. Under TPE condition (λ_{ex} = 800 nm), the FRET efficiency was measured as a function of porphyrin number, as a result, the average QD-porphyrin distance was obtained as 53 Å. $^1O_2$ generation of QD-porphyrin conjugates detected by disodium salt of 9,10-anthracenedipropionic acid (ADPA) and was 2 times more than that in porphyrin alone, which demonstrated high efficiency of QD-mediated photosensitization by TPE. Li *et al.* exploited TPE with CdTe QD-copper PC constructs.[63] E_{FRET} reached 44% when irradiated with a 780 nm femtosecond laser (200 mW). Higher irradiation power resulted in decreases of E_{FRET} because increased thermal motion of molecules can increase the distance between QD and PC, and TPE can promote electron transfer to upper excited states. ROS generation was not evaluated, although they suggested FRET phenomenon from QD to Pc by TPE. Valanciunaite *et al.* prepared CdSe/ZnS QDs bearing PEG-lipid coating to form non-covalent QD-Ce6 conjugates. They analyzed the FRET efficiency of QD-Ce6 conjugates by standard excitation (visible light) and TPE (830 nm).[64] They conjugated Ce6 molecules to QDs as molar ratios in the range from 0.1 to 10. QD-Ce6 conjugates (QD to Ce6 ratio = 1:5) showed E_{FRET} of ~60%; this high FRET suggests that QD is an efficient energy antenna in this system. They monitored E_{FRET} as a function of Ce6 amount, and estimated QD-to-Ce6 distance as 38–47 Å. This short distance suggested that the Ce6 molecules penetrated into the PEG-lipid coating on QD surface, which led to high E_{FRET}. They demonstrated the QD-Ce6 conjugates preserved high FRET efficiency (~50%) along with high stability inside living HeLa cells using two-photon fluorescence lifetime imaging microscopy (FLIM) measurement. This study provides a facile method to prepare robust QD-PS conjugates featuring efficient FRET. Although above Cd-based QDs demonstrated PDT effects, the Cd-induced cytotoxicity of the QDs is still problematic, and continuous efforts have been dedicated to produce Cd-free QDs for bioapplications including InP/ZnS,[65] $CuInS_2$[66] and $CuInS_2$/ZnS,[66b] Ag_2S[67] and Ag_2Se,[68] and ZnS-$AgInS_2$.[69] A recent review deeply discussed the current trend of Cd-free QDs and focused on their role for nanomedicine.[70] Charron *et al.* investigated Cd-free InP/ZnS QDs with reduced toxicity for PDT application created by QD FRET, which disclosed the underlying kinetics in $^1O_2$ generation of FRET-based QD-PS conjugates.[65b] InP/ZnS QDs (diameter = 2 – 3 nm) were coated by silica shell (thickness; 7 – 10 nm) and 5 – 20 of Ce6 were attached to each QD *via* covalent bond. They investigated systematically FRET kinetics in the various steps of the conjugate by means of optical spectroscopy. FRET from QD to Ce6 was confirmed as the rate-determining process for the generation of $^1O_2$, indicating that the FRET process significantly slows the Ce6 excitation. The conjugates showed the slower rate in $^1O_2$ production per Ce6, however, since many Ce6s were conjugated with the surface of QD, the overall $^1O_2$ production could increase. After UV irradiation for 5 min, QD-Ce6 conjugates incubated with breast cancer cells (MDA-

Author Manuscript Author Manuscript Author Manuscript Author Manuscript

MB-231) induced decrease of cell viability by 40% compared to Ce6 alone. This study emphasized that better chemical designs are essential to decrease the QD-PS spacing, which increases the FRET rate between QD and PS and overcomes the bottleneck problem. External excitation for PDT is a limitation toward clinical application because of poor tissue-penetration. In addition, the wavelength of irradiation should suit well for the absorption wavelength of PS in order to efficiently produce ROS. Hsu *et al.* used Renilla luciferase-immobilized QD (QD-RLuc8, λ_{em} of QD = 655 nm) for bioluminescence resonance energy transfer (BRET)-induced PDT to establish a self-illuminating QD system (Figure 7).[71] Carboxylated QDs were covalently bound to RLuc8 by amide bond formation *via* EDC chemistry. In the presence of coelenterazine, which is a substrate to activate RLuc8, the bioluminescence energy was transferred to QD with high possibility; the BRET efficiency, determined by integrated PL area ratio of RLuc8 to QD, reaching 0.92. In the presence of PS, Foscan™-embodied micelles, QD-RLuc8 plus coelenterazine generated ROS with QY of 40.8%, which killed significantly more A549 cells when compared with control groups. Furthermore, this system also effectively delayed tumor growth *in vivo*. This is an elegant method to overcome tissue penetration issue associated with external light sources. Yaghini *et al.* demonstrated that photochemical internalization (PCI), which uses PSs for photochemical rupture of vesical membranes to release materials confined in endosome and lysosome.[72] They functionalized CdSe/ZnS QDs (diameter < 10 nm) with amine-capped PEG and covalently conjugated QDs to the TAT peptides *via* EDC chemistry. A PS with negative charge, aluminum disulfonated phthalocyanine (AlPcS), was attached to the positively charged TAT-QD conjugate (diameter ~25 nm) by electrostatic interaction; R_0 value was calculated to be 59 Å. They investigated FRET from QD to AlPcS through the irradiation of 405 nm light using steady-state and time-resolved fluorescence spectroscopy, where QDs acted as donors and the AlPcSs mediated generation of $^1O_2$ as acceptors. The QY for $^1O_2$ generation was ~10%. In FLIM measurement, QD-AlPcS conjugates showed FRET-induced decrease in the lifetime of QD fluorescence even after the internalization into human breast carcinoma cells. QD excitation in the QD-AlPcS conjugates in cells induced the $^1O_2$ generation and led to intracellular redistribution of the conjugate from their initial endosomal and lysosomal localization, suggesting that the excitation promoted FRET from the QD to AlPcS with subsequent photooxidative damage of the vesicles.

5. Conclusions and Perspectives

QD-dye conjugates offer advantages for use in analytical, imaging, and therapeutic applications *via* FRET and/or eT mechanisms. Due to their outstanding optical properties of QDs and recent developments on numerous surface engineering for QD biocompatibility and for short and stable QD-dye linkage, QD-dye conjugates provide versatile platforms for sensing of cellular biomolecules, super-resolution fluorescence imaging based on photoactivatable or photoswitchable probes, and photodynamic therapeutics. Current studies have shown that QDs can be effectively employed as FRET and/or eT donors to dye molecules in QD-dye conjugate systems, with outstanding optical properties of QDs including narrow and symmetric emission and broad absorption spectra for multicolor signal or imaging. Especially, in FRET-based QD-dye conjugates, the accumulated studies in the past decade have established the calculation of the spectral overlap function and R_0, the

Author Manuscript Author Manuscript Author Manuscript Author Manuscript

experimental determination of E_{FRET}, and the estimation of QD-dye distance. There is, however, still a demand for enhanced dynamic range of fluorescence modulation for the practical use in the field of super-resolution imaging. In the aspect of therapeutics by QD-dye conjugates, unsettled problems exist such as long-term stability and clearance of QDs composed of toxic components. Biomedical community is moving towards the synthesis of non-toxic QDs and enhancement of tissue penetration depth for clinical applications. The final implementation is expected to rely on Cd-free QDs to reduce or eliminate the toxicity of heavy metal elements, and on the advancement of QD constructs to accomplish deep tissue imaging.

Acknowledgement

This work was supported by a grant from the KRIBB Research Initiative Program (Korean Biomedical Scientist Fellowship Program), Korea Research Institute of Bioscience and Biotechnology, Republic of Korea, and the Intramural Research Program (IRP), National Institute of Biomedical Imaging and Bioengineering (NIBIB), National Institutes of Health (NIH).

Biography

Dr. Sungwook Jung is a postdoctoral research fellow in the Laboratory of Molecular Imaging and Nanomedicine (LOMIN) of the National Institutes of Health (NIH). He received his Ph.D. in 2015 from the School of Interdisciplinary Bioscience and Bioengineering at Pohang University of Science and Technology (POSTECH). His research interests include QD conjugates for biosensing and super-resolution imaging, and nanomedicines for cancer therapy.

Prof. Xiaoyuan Chen majored in Chemistry and received his PhD from the University of Idaho in 1999. He became as an Assistant Professor in 2002 and moved to Stanford in 2004. He moved to NIH in 2009 as a Senior Investigator and the Chief of the Laboratory of Molecular Imaging and Nanomedicine (LOMIN) at the National Institute of Biomedical Imaging and Bioengineering (NIBIB) of NIH. His research interests include development of a molecular imaging toolbox for a better understanding of biology, early diagnosis of disease, monitoring the therapy response, and guiding drug discovery/development. His lab puts special emphasis on high-sensitivity nanosensors for biomarker detection and theranostic nanomedicine for imaging, gene and drug delivery, and monitoring of treatment.

Author Manuscript Author Manuscript Author Manuscript Author Manuscript

References

[1]. a) Medintz IL, Uyeda HT, Goldman ER, Mattoussi H, Nat Mater 2005, 4, 435; [PubMed: 15928695] b) Michalet X, Pinaud FF, Bentolila LA, Tsay JM, Doose S, Li JJ, Sundaresan G, Wu AM, Gambhir SS, Weiss S, Science 2005, 307, 538. [PubMed: 15681376]

[2]. a) Bruchez M, Moronne M, Gin P, Weiss S, Alivisatos AP, Science 1998, 281, 2013; [PubMed: 9748157] b) Chan WCW, Nie S, Science 1998, 281, 2016; [PubMed: 9748158] c) Jaiswal JK, Mattoussi H, Mauro JM, Simon SM, Nat. Biotechnol 2003, 21, 47. [PubMed: 12459736]

[3]. a) Dahan M, Lévi S, Luccardini C, Rostaing P, Riveau B, Triller A, Science 2003, 302, 442; [PubMed: 14564008] b) Courty S, Luccardini C, Bellaiche Y, Cappello G, Dahan M, Nano Lett. 2006, 6, 1491; [PubMed: 16834436] c) Zhang R, Rothenberg E, Fruhwirth G, Simonson PD, Ye F, Golding I, Ng T, Lopes W, Selvin PR, Nano Lett. 2011, 11, 4074. [PubMed: 21882883]

[4]. a) Cai W, Shin D-W, Chen K, Gheysens O, Cao Q, Wang SX, Gambhir SS, Chen X, Nano Lett. 2006, 6, 669; [PubMed: 16608262] b) Kim S, Lim YT, Soltesz EG, De Grand AM, Lee J, Nakayama A, Parker JA, Mihaljevic T, Laurence RG, Dor DM, Cohn LH, Bawendi MG, Frangioni JV, Nat Biotech 2004, 22, 93;c) Gao X, Cui Y, Levenson RM, Chung LWK, Nie S, Nat Biotech 2004, 22, 969;d) Kobayashi H, Hama Y, Koyama Y, Barrett T, Regino CAS, Urano Y, Choyke PL, Nano Lett. 2007, 7, 1711. [PubMed: 17530812]

[5]. Clapp AR, Pons T, Medintz IL, Delehanty JB, Melinger JS, Tiefenbrunn T, Dawson PE, Fisher BR, O'Rourke B, Mattoussi H, Advanced Materials 2007, 19, 1921.

[6]. Sapsford KE, Algar WR, Berti L, Gemmill KB, Casey BJ, Oh E, Stewart MH, Medintz IL, Chem. Rev 2013, 113, 1904. [PubMed: 23432378]

[7]. van der Meer BW, in FRET – Förster Resonance Energy Transfer, DOI: 10.1002/9783527656028.ch03, Wiley-VCH Verlag GmbH & Co. KGaA 2013, p. 23.

[8]. Algar WR, Kim H, Medintz IL, Hildebrandt N, Coordination Chemistry Reviews 2014, 263–264, 65.

[9]. Clapp AR, Medintz IL, Mauro JM, Fisher BR, Bawendi MG, Mattoussi H, J. Am. Chem. Soc 2004, 126, 301. [PubMed: 14709096]

[10]. in Principles of Fluorescence Spectroscopy, DOI: 10.1007/978-0-387-46312-4_8 (Ed: Lakowicz JR), Springer US, Boston, MA 2006, p. 277.

[11]. a) Rogach AL, Klar TA, Lupton JM, Meijerink A, Feldmann J, J. Mat. Chem 2009, 19, 1208;b) Medintz IL, Mattoussi H, Phys. Chem. Chem. Phys 2009, 11, 17. [PubMed: 19081907]

[12]. a) Marcus RA, J. Chem. Phys. 1956, 24, 966;b) Marcus RA, Annu. Rev. Phys. Chem 1964, 15, 155;c) Marcus RA, J. Chem. Phys 1956, 24, 979.

[13]. Tavernier HL, Fayer MD, J. Phys. Chem. B 2000, 104, 11541.

[14]. Harris RD, Bettis Homan S, Kodaimati M, He C, Nepomnyashchii AB, Swenson NK, Lian S, Calzada R, Weiss EA, Chem. Rev 2016, 116, 12865. [PubMed: 27499491]

[15]. a) Medintz IL, Farrell D, Susumu K, Trammell SA, Deschamps JR, Brunel FM, Dawson PE, Mattoussi H, Anal. Chem 2009, 81, 4831; [PubMed: 19445483] b) Jung S, Park J, Bang J, Kim J-Y, Kim C, Jeon Y, Lee SH, Jin H, Choi S, Kim B, Lee WJ, Pack C-G, Lee J-B, Lee NK, Kim S, J. Am. Chem. Soc 2017, 139, 7603. [PubMed: 28493679]

[16]. Algar WR, Stewart MH, Scott AM, Moon WJ, Medintz IL, J. Mater. Chem. B 2014, 2, 7816.

[17]. a) Stewart MH, Huston AL, Scott AM, Oh E, Algar WR, Deschamps JR, Susumu K, Jain V, Prasuhn DE, Blanco-Canosa J, Dawson PE, Medintz IL, ACS Nano 2013, 7, 9489; [PubMed: 24128175] b) Sandros MG, Gao D, Benson DE, J. Am. Chem. Soc 2005, 127, 12198; [PubMed: 16131178] c) Stewart MH, Huston AL, Scott AM, Efros AL, Melinger JS, Gemmill KB, Trammell SA, Blanco-Canosa JB, Dawson PE, Medintz IL, ACS Nano 2012, 6, 5330; [PubMed:

Author Manuscript Author Manuscript Author Manuscript Author Manuscript

22671940] d) Jeong S, Song J, Lee W, Ryu YM, Jung Y, Kim S-Y, Kim K, Hong SC, Myung SJ, Kim S, Nano Letters 2017, 17, 1378. [PubMed: 28125238]

[18]. Hamm LL, Nakhoul N, Hering-Smith KS, Clin. J. Am. Soc. Nephrol 2015, 10, 2232. [PubMed: 26597304]

[19]. Tortora GJ, Derrickson B, Principles of anatomy & physiology, Wiley, Hoboken, NJ 2012.

[20]. a) Medintz IL, Stewart MH, Trammell SA, Susumu K, Delehanty JB, Mei BC, Melinger JS, Blanco-Canosa JB, Dawson PE, Mattoussi H, Nat. Mater 2010, 9, 676; [PubMed: 20651808] b) Susumu K, Field LD, Oh E, Hunt M, Delehanty JB, Palomo V, Dawson PE, Huston AL, Medintz IL, Chem. Mater 2017, 29, 7330;c) Tang R, Lee H, Achilefu S, J. Am. Chem. Soc 2012, 134, 4545; [PubMed: 22360301] d) Snee PT, Somers RC, Nair, Zimmer JP, Bawendi MG, Nocera DG, J. Am. Chem. Soc 2006, 128, 13320; [PubMed: 17031920] e) Krooswyk JD, Tyrakowski CM, Snee PT, J. Phys. Chem. C 2010, 114, 21348;f) Dennis AM, Rhee WJ, Sotto D, Dublin SN, Bao G, ACS Nano 2012, 6, 2917. [PubMed: 22443420]

[21]. Berezin Mikhail Y., Guo K, Akers W, Northdurft Ralph E., Culver Joseph P., Teng B, Vasalatiy O, Barbacow K, Gandjbakhche A, Griffiths Gary L., Achilefu S, Biophysical Journal 2011, 100, 2063. [PubMed: 21504743]

[22]. a) Hu B, Hu L-L, Chen M-L, Wang J-H, Biosensors and Bioelectronics 2013, 49, 499; [PubMed: 23811485] b) Wu L, Guo Q-S, Liu Y-Q, Sun Q-J, Anal. Chem 2015, 87, 5318; [PubMed: 25932651] c) Zamaleeva AI, Collot M, Bahembera E, Tisseyre C, Rostaing P, Yakovlev AV, Oheim M, de Waard M, Mallet J-M, Feltz A, Nano Lett. 2014, 14, 2994; [PubMed: 24754795] d) Wang Y, Mao H, Wong LB, Talanta 2011, 85, 694. [PubMed: 21645760]

[23]. Helmlinger G, Yuan F, Dellian M, Jain RK, Nat. Med 1997, 3, 177. [PubMed: 9018236]

[24]. Vaupel P, Kallinowski F, Okunieff P, Cancer Res. 1989, 49, 6449. [PubMed: 2684393]

[25]. McLaurin EJ, Greytak AB, Bawendi MG, Nocera DG, J. Am. Chem. Soc 2009, 131, 12994. [PubMed: 19697933]

[26]. Ingram JM, Zhang C, Xu J, Schiff SJ, J Neurosci Methods 2013, 214, 45. [PubMed: 23333398]

[27]. Freeman R, Gill R, Shweky I, Kotler M, Banin U, Willner I, Angewandte Chemie International Edition 2009, 48, 309. [PubMed: 19053111]

[28]. Shi L, De Paoli V, Rosenzweig N, Rosenzweig Z, J. Am. Chem. Soc 2006, 128, 10378. [PubMed: 16895398]

[29]. Chung EY, Ochs CJ, Wang Y, Lei L, Qin Q, Smith AM, Strongin AY, Kamm R, Qi Y-X, Lu S, Wang Y, Nano Lett. 2015, 15, 5025. [PubMed: 26203778]

[30]. a) Smith AM, Mancini MC, Nie S, Nat. Nanotechnol 2009, 4, 710; [PubMed: 19898521] b) Won N, Jeong S, Kim K, Kwag J, Park J, Kim SG, Kim S, Molecular imaging 2012, 11, 338. [PubMed: 22954148]

[31]. Field LD, Delehanty JB, Chen Y, Medintz IL, Acc. Chem. Res 2015, 48, 1380. [PubMed: 25853734]

[32]. Hou Y, Guo Z, Li J, Wang PG, Biochem. Biophys. Res. Commun 1996, 228, 88. [PubMed: 8912640]

[33]. Deneke SM, in Current Topics in Cellular Regulation, Vol. 36 (Eds: Stadtman ER, Chock PB), Academic Press 2001, p. 151.

[34]. a) Gui R, An X, Su H, Shen W, Zhu L, Ma X, Chen Z, Wang X, Talanta 2012, 94, 295; [PubMed: 22608451] b) Han B, Yuan J, Wang E, Anal. Chem 2009, 81, 5569; [PubMed: 19499913] c) Banerjee S, Kar S, Perez JM, Santra S, J. Phys. Chem. C 2009, 113, 9659;d) Liu J, Bao C, Zhong X, Zhao C, Zhu L, Chem. Commun 2010, 46, 2971.

[35]. a) Pencheva N, Tavazoie SF, Nat. Cell Biol 2013, 15, 546; [PubMed: 23728460] b) Calin GA, Croce CM, Nat. Rev. Cancer 2006, 6, 857. [PubMed: 17060945]

[36]. Mestdagh P, Hartmann N, Baeriswyl L, Andreasen D, Bernard N, Chen C, Cheo D, D'Andrade P, DeMayo M, Dennis L, Derveaux S, Feng Y, Fulmer-Smentek S, Gerstmayer B, Gouffon J, Grimley C, Lader E, Lee KY, Luo S, Mouritzen P, Narayanan A, Patel S, Peiffer S, Rüberg S, Schroth G, Schuster D, Shaffer JM, Shelton EJ, Silveria S, Ulmanella U, Veeramachaneni V, Staedtler F, Peters T, Guettouche T, Wong L, Vandesompele J, Nat. Meth 2014, 11, 809.

[37]. a) Qiu X, Hildebrandt N, ACS Nano 2015, 9, 8449; [PubMed: 26192765] b) Su S, Fan J, Xue B, Yuwen L, Liu X, Pan D, Fan C, Wang L, ACS Appl. Mater. Interfaces 2014, 6, 1152; [PubMed:

Author Manuscript Author Manuscript Author Manuscript Author Manuscript

24380365] c) Jiang G, Susha AS, Lutich AA, Stefani FD, Feldmann J, Rogach AL, ACS Nano 2009, 3, 4127; [PubMed: 19928994] d) Samanta A, Buckhout-White S, Oh E, Susumu K, Medintz IL, Mol. Syst. Des. Eng 2018, 3, 314.

[38]. Hoyer P, Staudt T, Engelhardt J, Hell SW, Nano Letters 2011, 11, 245. [PubMed: 21128678]

[39]. a) Dertinger T, Colyer R, Iyer G, Weiss S, Enderlein J, P Natl Acad Sci USA 2009, 106, 22287;b) Dertinger T, Colyer R, Vogel R, Enderlein J, Weiss S, Opt Express 2010, 18, 18875. [PubMed: 20940780]

[40]. a) Nirmal M, Dabbousi BO, Bawendi MG, Macklin JJ, Trautman JK, Harris TD, Brus LE, Nature 1996, 383, 802b) Frantsuzov PA, Marcus RA, Phys Rev B 2005, 72.

[41]. a) Qin HY, Shang XJ, Ning ZJ, Fu T, Niu ZC, Brismar H, Agren H, Fu Y, J Phys Chem C 2012, 116, 12786;b) Hefti R, Jones M, Moyer PJ, J Phys Chem C 2012, 116, 25617.

[42]. Fernandez-Suarez M, Ting AY, Nat Rev Mol Cell Biol 2008, 9, 929. [PubMed: 19002208]

[43]. a) Yildiz I, Deniz E, Raymo FM, Chemical Society Reviews 2009, 38, 1859; [PubMed: 19551167] b) Credi A, New J. Chem. 2012, 36, 1925.

[44]. Zhu L, Zhu M-Q, Hurst JK, Li ADQ, J. Am. Chem. Soc 2005, 127, 8968. [PubMed: 15969571]

[45]. Díaz SA, Gillanders F, Jares-Erijman EA, Jovin TM, Nat. Commun 2015, 6, 6036. [PubMed: 25592060]

[46]. a) Impellizzeri S, McCaughan B, Callan JF, Raymo FM, J. Am. Chem. Soc 2012, 134, 2276; [PubMed: 22217330] b) Han G, Mokari T, Ajo-Franklin C, Cohen BE, J. Am. Chem. Soc 2008, 130, 15811. [PubMed: 18983148]

[47]. Tagliazucchi M, Amin VA, Schneebeli ST, Stoddart JF, Weiss EA, Advanced Materials 2012, 24, 3617. [PubMed: 22678816]

[48]. Bang J, Chon B, Won N, Nam J, Joo T, Kim S, J. Phys. Chem. C 2009, 113, 6320.

[49]. Bang J, Park J, Velu R, Yoon E, Lee K, Cho S, Cha S, Chae G, Joo T, Kim S, Chem. Commun 2012, 48, 9174.

[50]. Jha PP, Guyot-Sionnest P, J. Phys. Chem. C 2007, 111, 15440.

[51]. a) Dougherty TJ, Journal of clinical laser medicine & surgery 1996, 14, 219; [PubMed: 9612186] b) Samia ACS, Dayal S, Burda C, Photochem. Photobiol 2006, 82, 617. [PubMed: 16475871]

[52]. a) Dai Y, Xu C, Sun X, Chen X, Chem. Soc. Rev 2017, 46, 3830; [PubMed: 28516983] b) Fan W, Huang P, Chen X, Chem. Soc. Rev 2016, 45, 6488; [PubMed: 27722560] c) Zhou Z, Song J, Nie L, Chen X, Chem. Soc. Rev 2016, 45, 6597; [PubMed: 27722328] d) Zhou Z, Song J, Tian R, Yang Z, Yu G, Lin L, Zhang G, Fan W, Zhang F, Niu G, Nie L, Chen X, Angewandte Chemie International Edition 2017, 56, 6492; [PubMed: 28470979] e) Tong X, Srivatsan A, Jacobson O, Wang Y, Wang Z, Yang X, Niu G, Kiesewetter DO, Zheng H, Chen X, Sci. Rep 2016, 6, 31551; [PubMed: 27546160] f) Han K, Zhang J, Zhang W, Wang S, Xu L, Zhang C, Zhang X, Han H, ACS Nano 2017, 11, 3178; [PubMed: 28296387] g) Dong H, Tang S, Hao Y, Yu H, Dai W, Zhao G, Cao Y, Lu H, Zhang X, Ju H, ACS Appl. Mater. Interfaces 2016, 8, 3107. [PubMed: 26761391]

[53]. Moan J, Berg K, Photochem. Photobiol 1991, 53, 549. [PubMed: 1830395]

[54]. Hone DC, Walker PI, Evans-Gowing R, FitzGerald S, Beeby A, Chambrier I, Cook MJ, Russell DA, Langmuir 2002, 18, 2985.

[55]. Roy I, Ohulchanskyy TY, Pudavar HE, Bergey EJ, Oseroff AR, Morgan J, Dougherty TJ, Prasad PN, J. Am. Chem. Soc 2003, 125, 7860. [PubMed: 12823004]

[56]. a) Samia ACS, Chen X, Burda C, J. Am. Chem. Soc 2003, 125, 15736; [PubMed: 14677951] b) Bakalova R, Ohba H, Zhelev Z, Ishikawa M, Baba Y, Nat. Biotechnol 2004, 22, 1360; [PubMed: 15529155] c) Bakalova R, Ohba H, Zhelev Z, Nagase T, Jose R, Ishikawa M, Baba Y, Nano Lett. 2004, 4, 1567.

[57]. Alivisatos P, in Pure and Applied Chemistry, Vol. 72, 2000, 3.

[58]. Li Y-S, Zaidi SIA, Rodgers MAJ, Mukhtar H, Kenney ME, Oleinick NL, He J, Larkin HE, Rihter BD, Photochem. Photobiol 1997, 65, 581. [PubMed: 9077144]

[59]. Yaghini E, Pirker KF, Kay CWM, Seifalian AM, MacRobert AJ, Small 2014, 10, 5106. [PubMed: 25164061]

[60]. Shi L, Hernandez B, Selke M, J. Am. Chem. Soc 2006, 128, 6278. [PubMed: 16683767]

Author Manuscript Author Manuscript Author Manuscript Author Manuscript

[61]. Tsay JM, Trzoss M, Shi L, Kong X, Selke M, Jung ME, Weiss S, J. Am. Chem. Soc 2007, 129, 6865. [PubMed: 17477530]

[62]. Qi Z-D, Li D-W, Jiang P, Jiang F-L, Li Y-S, Liu Y, Wong W-K, Cheah K-W, J. Mat. Chem 2011, 21, 2455.

[63]. Li F, He Z, Li M, Zhang J, Han J, Lu P, Mater. Lett 2014, 132, 263.

[64]. Valanciunaite J, Klymchenko AS, Skripka A, Richert L, Steponkiene S, Streckyte G, Mely Y, Rotomskis R, RSC Adv. 2014, 4, 52270.

[65]. a) Thomas A, Nair PV, George Thomas K, J. Phys. Chem. C 2014, 118, 3838;b) Charron G, Stuchinskaya T, Edwards DR, Russell DA, Nann T, J. Phys. Chem. C 2012, 116, 9334.

[66]. a) Kolny-Olesiak J, Weller H, ACS Appl. Mater. Interfaces 2013, 5, 12221; [PubMed: 24187935] b) Zhang W, Lou Q, Ji W, Zhao J, Zhong X, Chem. Mater 2014, 26, 1204.

[67]. a) Gui R, Wan A, Liu X, Yuan W, Jin H, Nanoscale 2014, 6, 5467; [PubMed: 24728046] b) Gao J, Wu C, Deng D, Wu P, Cai C, Adv. Healthcare Mater 2016, 5, 2437.

[68]. Zhu C-N, Jiang P, Zhang Z-L, Zhu D-L, Tian Z-Q, Pang D-W, ACS Appl. Mater. Interfaces 2013, 5, 1186. [PubMed: 23380909]

[69]. Regulacio MD, Win KY, Lo SL, Zhang S-Y, Zhang X, Wang S, Han M-Y, Zheng Y, Nanoscale 2013, 5, 2322. [PubMed: 23392168]

[70]. Xu G, Zeng S, Zhang B, Swihart MT, Yong K-T, Prasad PN, Chem. Rev 2016, 116, 12234. [PubMed: 27657177]

[71]. Hsu C-Y, Chen C-W, Yu H-P, Lin Y-F, Lai P-S, Biomaterials 2013, 34, 1204. [PubMed: 23069718]

[72]. Yaghini E, Giuntini F, Eggleston IM, Suhling K, Seifalian AM, MacRobert AJ, Small 2014, 10, 782. [PubMed: 24031023]

Author Manuscript Author Manuscript Author Manuscript Author Manuscript

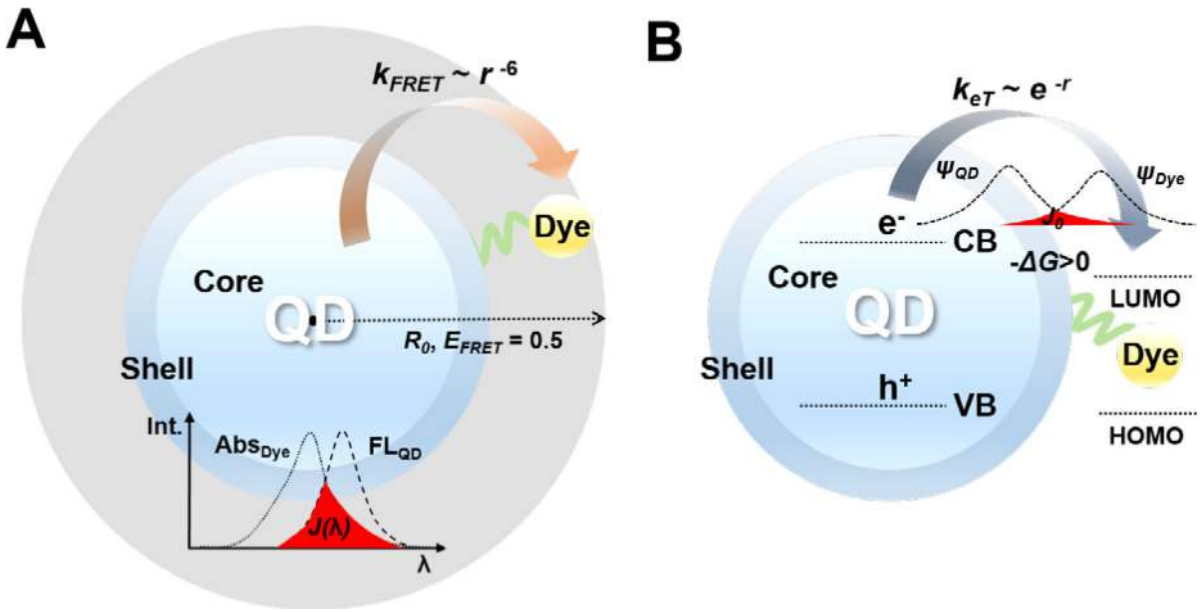

Figure 1.

A) A FRET construct which consists of QD and dye. Förster distance (R_0) determined from the center of QD, indicating how FRET is effective. (*e.g.*, E_{FRET} = 0.5 at R_0). Absorbance (Abs) of the dye spectrally overlaps with fluorescence (FL) of QD, as indicated by a red colored area. The spectral overlap is denoted as $J(\lambda)$. The FRET rate (k_{FRET}) relies on the QD-dye distance (r) as a factor of –6. B) An eT construct which consists of QD and dye. The dye has the lowest unoccupied molecular orbital (LUMO) level between the $1S_h$ and $1S_e$ band-edge states of the QD, inducing positive value of driving force ($-\Delta G > 0$). The electron orbital of dye overlaps with the electron orbital of the QD, denoted as a red colored area. The orbital overlap is associated with the electronic coupling matrix element (J_0). These satisfied requirements enable eT from QD to dye. The eT rate (k_{eT}) decreases exponentially as increasing r. CB: conduction band. VB: valence band. HOMO highest occupied molecular orbital.

Author Manuscript Author Manuscript Author Manuscript Author Manuscript

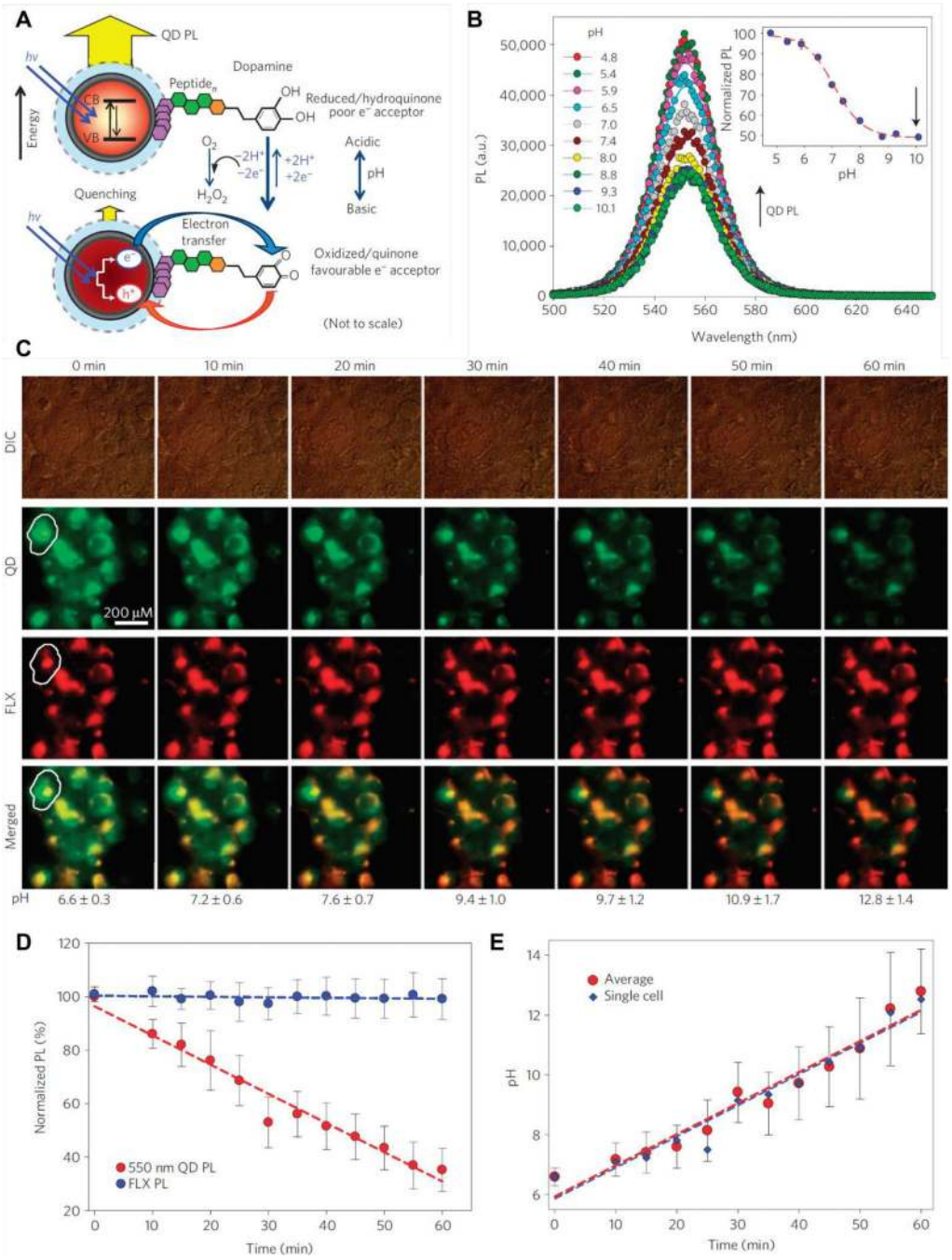

Figure 2.

A) A scheme for pH sensitive QD-dopamine conjugates. In the solution with low pH, dominant form of dopamine is hydroquinone which poorly accepts electrons from QD, inducing low photoluminescence (PL) quenching of QD. With increasing pH, O_2 oxidizes dopamine, inducing an increase of quinone concentration which a favourable electron acceptor or QD. B) Fluorescence spectra measured from QD-dopamine conjugates in the buffer with pH 10.1 and with lower pH. Inset: A plot of the fluorescence recovery beginning from pH 10.1 (arrow). C) Bright-field and fluorescence microscope images taken from

Author Manuscript Author Manuscript Author Manuscript Author Manuscript

COS-1 cells injected with QD-dopamine conjugates and FLX nanospheres in pH 6.5 PBS. Medium was switched to pH 11.5 PBS and images were taken at the indicated time intervals. D) QD and FLX fluorescence from the images plotted in C as a function of incubation time. E) Average pH values derived from the fluorescence data (D). Single cell case is well correlated with average values. Reproduced from permission.[20a] Copyright 2010 Nature Publishing Group.

Author Manuscript Author Manuscript Author Manuscript Author Manuscript

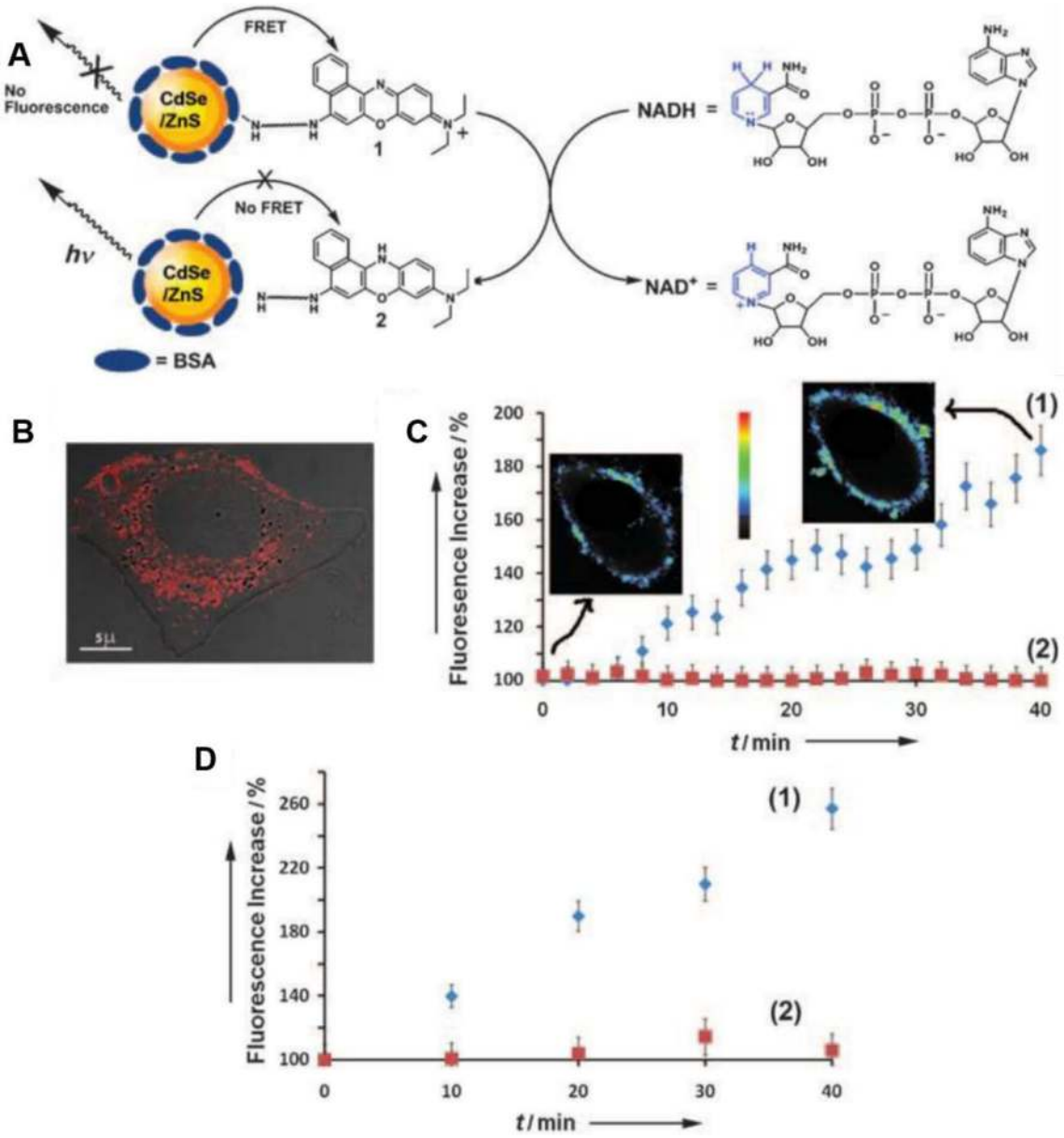

Figure 3.

A) A scheme for sensing of NADH by QD-NB conjugates. B) Confocal fluorescence microscope image of a HeLa cell incubated with QD-NB conjugates. C) (1) Change of fluorescence intensities from HeLa cells incubated with QD-NB conjugates upon interaction with D-glucose (1) or L-glucose (2). Inset: The fluorescence image of a representative cell before and after the addition of D-glucose. D) Change of fluorescence intensities of HeLa cells incubated with QD-NB conjugates in the presence of D-glucose to HeLa cells (1), and taxol-treated HeLa cells (2). Reproduced from permission.[27] Copyright 2008 John Wiley and Sons.

Author Manuscript
Author Manuscript
Author Manuscript
Author Manuscript

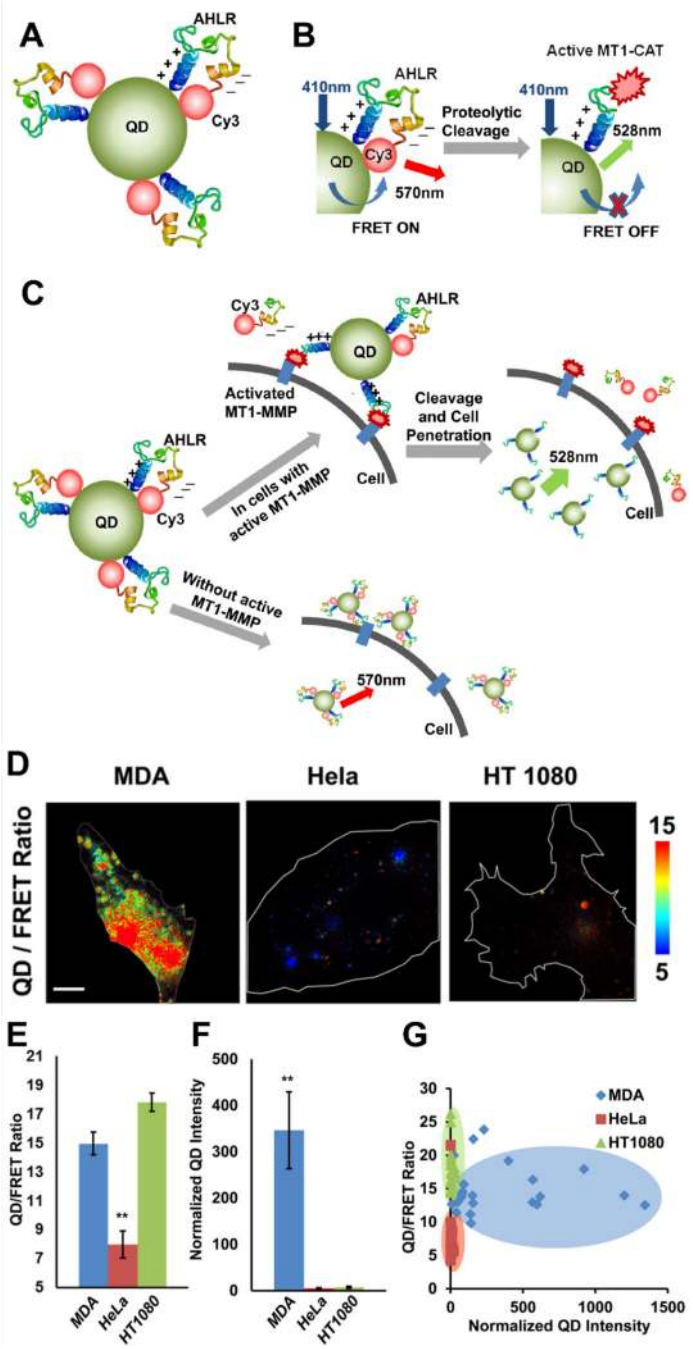

Figure 4.

A) A scheme for QD-Cy3 conjugates possessing bent peptides which allow a high FRET between the QD and Cy3. B) A scheme for activation mechanism of QD-Cy3 conjugates upon the cleavage by MMP protease (MT1-CAT). C) A scheme for activation of QD-Cy3 conjugates in cancer cells with active MT1-MMP, and triggered penetration into the cells. D) Representative QD/FRET ratio images of MDA-MB-231, HeLa, and HT1080 cell. E) Comparison of the QD/FRET ratio and QD intensity of MDA-MB-231, HeLa, and HT1080. **: $p < 0.001$. F) A 2D plot for QD intensity (x axis) and QD/FRET ratio (y axis) from

MDA-MB-231 (blue), HeLa (red), and HT1080 (green) cells. Reproduced from permission.[29] Copyright 2015 American Chemical Society.

Author Manuscript Author Manuscript Author Manuscript Author Manuscript

Author Manuscript Author Manuscript Author Manuscript Author Manuscript

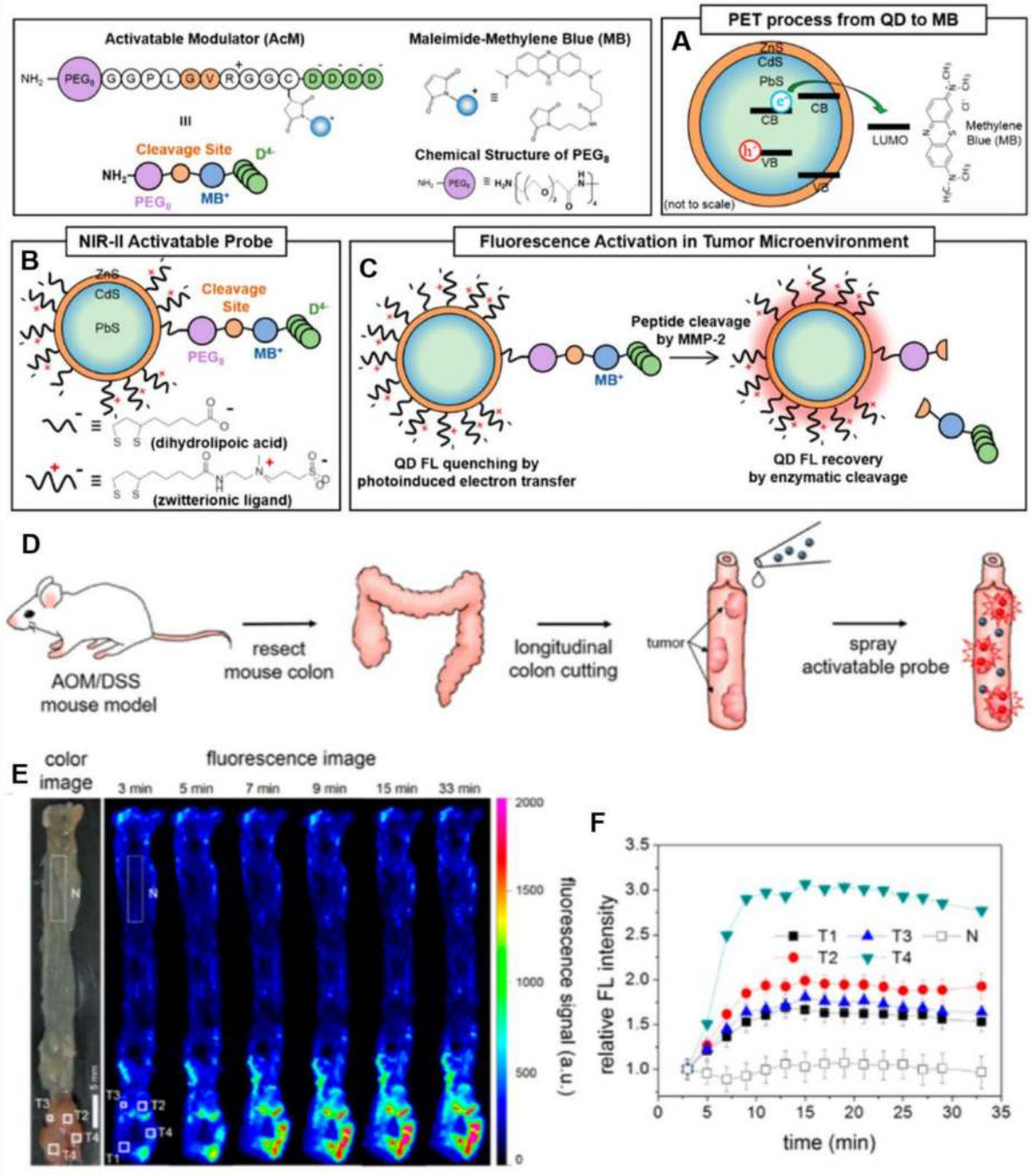

Figure 5.

A) A scheme for eT from QD to methylene blue (MB). B) A scheme for the surface design of a QD to confer protease-activation. C) Release of the electron donor, MB, from the surface of the QD under the enzymatic reaction. D) A scheme for ex vivo fluorescence imaging in mouse colon model by QD-MB conjugates. A colon was obtained in a mouse treated with AOM/DSS and QD-MB conjugates was sprayed to the colon. (E) Ex vivo fluorescence imaging of colon tumor by sprayed QD-MB conjugates. T1–T4: tumor region,

Author Manuscript Author Manuscript Author Manuscript Author Manuscript

N: normal colon tissue. (F) Fluorescence signals of the selected region as a function of time. Reproduced from permission.[17d] Copyright 2017 American Chemical Society.

Author Manuscript Author Manuscript Author Manuscript Author Manuscript

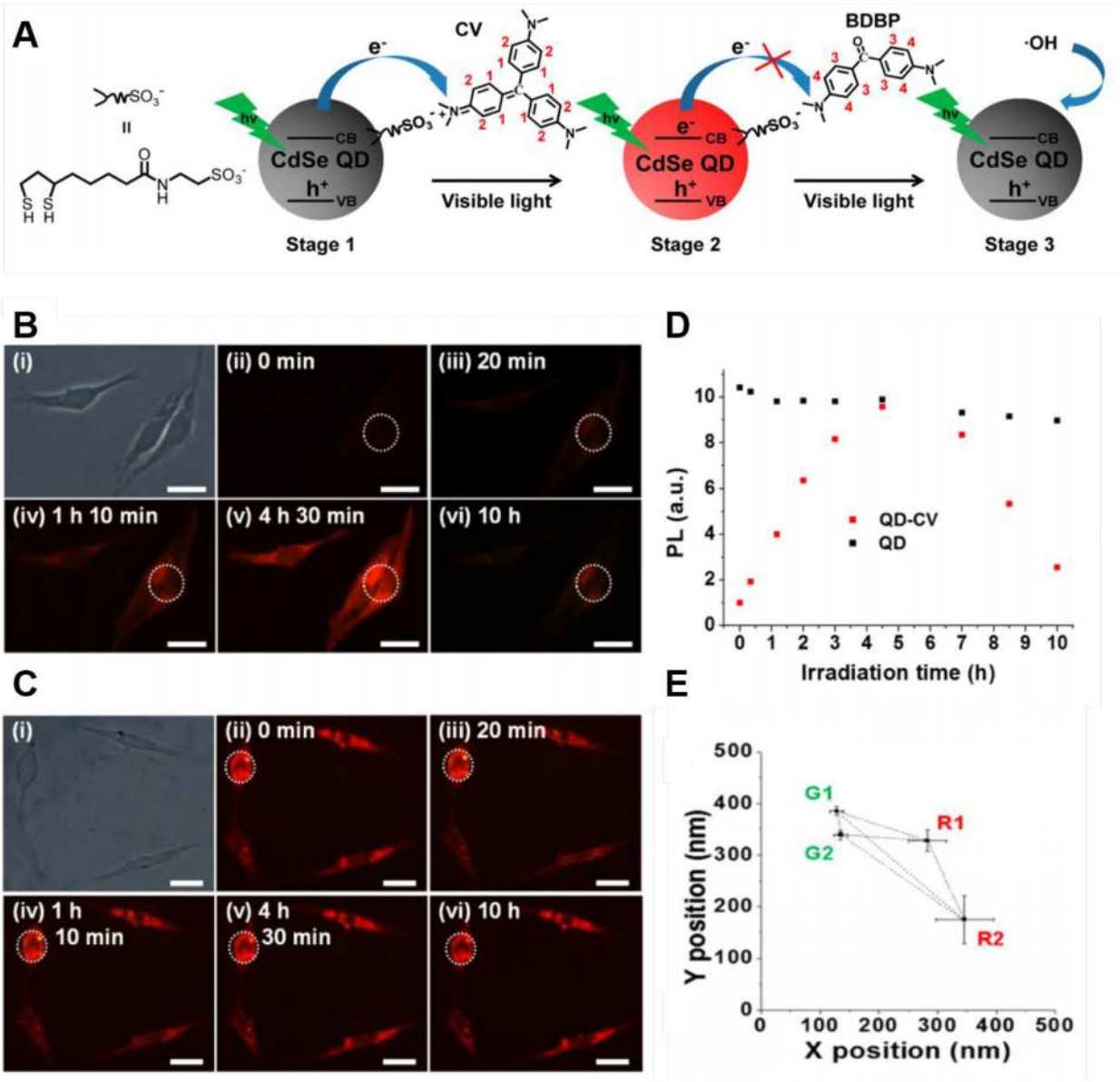

Figure 6.

A) A scheme for fluorescence modulation of a QD-CV conjugates. B) HeLa cells incubated with QD-CV conjugates (i) bright-field image abtained after 2 h of incubation. Fluorescence images were taken after irradiation of blue light (11 mW/cm^2) for 0 – 10 h (ii – vi). Scale bars: 20 μm. C) Unconjugated QD incubated with the cells as a control group D) Fluorescence intensities from cells incubated with the QD-CV conjugates or the unconjugated QDs over irradiation time. White dotted circles: regions of interest. E) Colocalizations of the four QD-CV conjugates in a synchronized coordinate system. G: QD with green emission. R: QD with red emission. Reproduced from permission.[15b] Copyright 2017 American Chemical Society.

Author Manuscript Author Manuscript Author Manuscript Author Manuscript

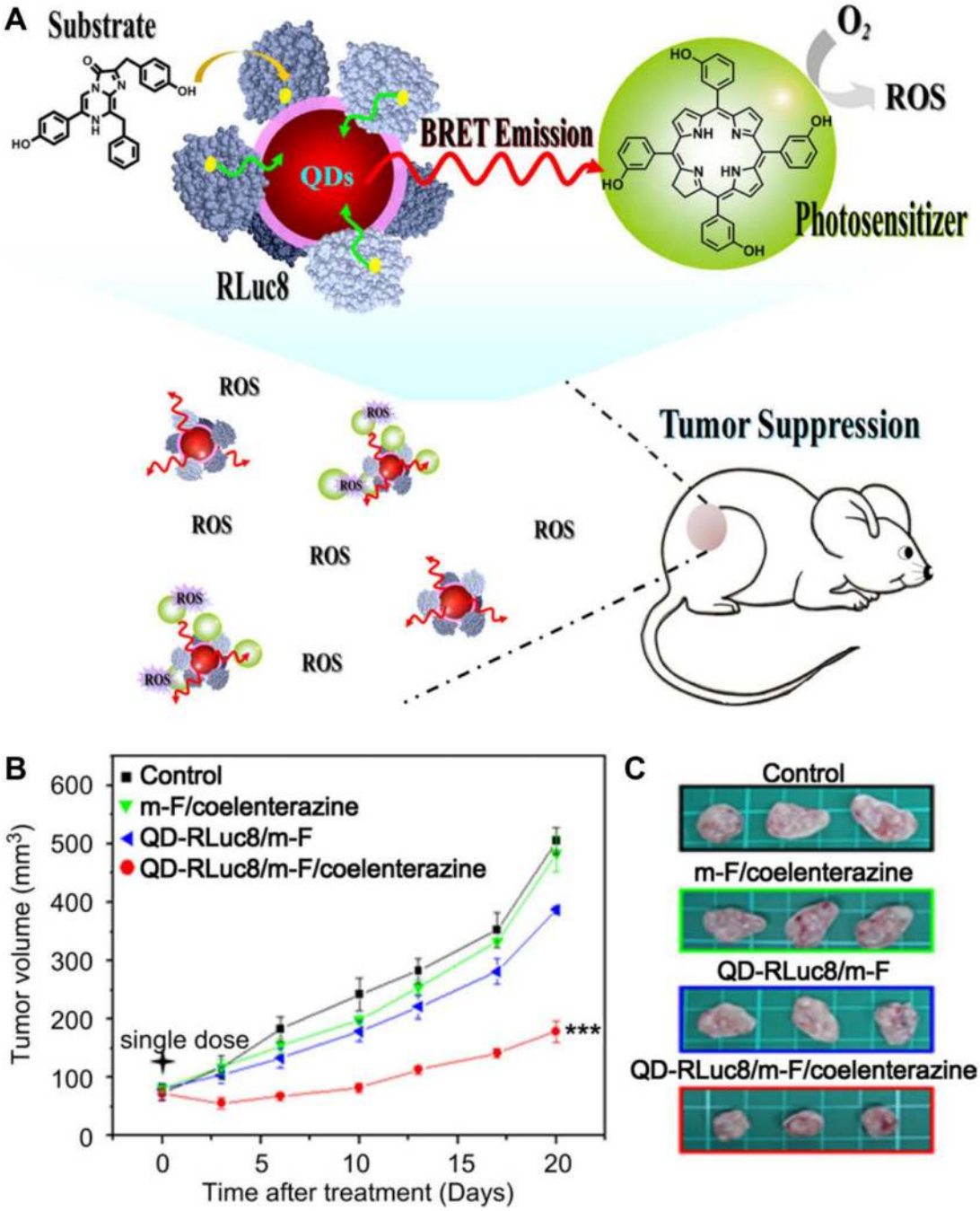

Figure 7.

A) A scheme for bioluminescence resonance energy transfer (BRET) to induce PDT in QD-RLuc8 conjugates. B) Curves of tumor (A549) growth after the treatment of QD-RLuc8 conjugates (10 pmol) and control groups. m-F: Foscan-loaded micelle. ***: $p < 0.0001$. Reproduced from permission.[71] Copyright 2013 Elsevier.